

## MIT Open Access Articles

*Resource recovery from desalination brine: energy efficiency and purification process integration for sodium hydroxide production*

The MIT Faculty has made this article openly available. **Please share** how this access benefits you. Your story matters.

**Citation:** F. Du et al. "Sodium hydroxide production from seawater desalination brine: process design and energy efficiency," *Environmental Science & Technology*, 52, 10 (April 2018): 5949–5958 © 2018 American Chemical Society

**As Published:** <http://dx.doi.org/10.1021/acs.est.8b01195>

**Publisher:** American Chemical Society (ACS)

**Persistent URL:** <https://hdl.handle.net/1721.1/123096>

**Version:** Author's final manuscript: final author's manuscript post peer review, without publisher's formatting or copy editing

**Terms of Use:** Article is made available in accordance with the publisher's policy and may be subject to US copyright law. Please refer to the publisher's site for terms of use.



# Resource recovery from desalination brine: energy efficiency and purification process integration for sodium hydroxide production

*Fengmin Du<sup>a</sup>, David M. Warsinger<sup>a</sup>, Tamanna I. Urmi<sup>a</sup>, Gregory P. Thiel<sup>a</sup>, Amit Kumar<sup>a</sup>, and*

*John H Lienhard V<sup>a\*</sup>*

<sup>a</sup>Rohsenow Kendall Heat Transfer Laboratory, Department of Mechanical Engineering Massachusetts Institute of Technology, 77 Massachusetts Avenue, Cambridge MA 02139-4307 USA

## ABSTRACT

The ability to increase pH is a crucial need for desalination pretreatment (especially in reverse osmosis) and for other industries, but processes used to raise pH often incur significant emissions and non-renewable resource use. Alternatively, waste brine from desalination can be used to create sodium hydroxide, via appropriate concentration and purification pretreatment steps, for input into the chlor-alkali process. In this work, an efficient process train (with variations) is developed and modeled for sodium hydroxide production from seawater desalination brine using membrane chlor-alkali electrolysis. The integrated system includes nanofiltration, concentration via evaporation or mechanical vapor compression, chemical softening, further ion-exchange softening, dechlorination, and membrane electrolysis. System productivity, component performance, and energy consumption of the NaOH production process are highlighted, and their dependencies on electrolyzer outlet conditions

19 and brine recirculation are investigated. The analysis of the process also includes assessment of the  
20 energy efficiency of major components, estimation of system operating expense and comparison with  
21 similar processes. The brine-to-caustic process is shown to be technically feasible while offering several  
22 advantages, i.e. the reduced environmental impact of desalination through lessened brine discharge,  
23 and the increase in the overall water recovery ratio of the reverse osmosis facility. Additionally, best-  
24 use conditions are given for producing caustic not only for use within the plant, but also in excess  
25 amounts for potential revenue.

## 26 INTRODUCTION

27 As the global population grows and economies develop, demands on the world's fixed fresh water  
28 supply are increasing. Both the growing demand and regional water stress—often punctuated by a  
29 changing climate—are driving the rising use of seawater desalination to access the 97% of Earth's  
30 water found in the oceans.<sup>1</sup> With considerable reductions in energy consumption and cost over the  
31 past several decades, the dominant choice for new seawater desalination facilities is reverse osmosis  
32 (RO).<sup>2</sup>

33 Due to the implementation of more energy-efficient pumps and improved membranes, RO processes  
34 are coming closer to the thermodynamic minimum energy consumption.<sup>3,4</sup> Despite these technological  
35 advances, however, seawater RO (SWRO) – and all desalination systems currently in use today –  
36 produce a large quantity of concentrated brine that is discharged back to the sea.<sup>5</sup> This discharge has  
37 been reported to threaten marine ecosystems<sup>6</sup> in several ways, including upsetting the physiochemical  
38 balance, causing thermal plumes, and amplifying contaminant concentration.<sup>7</sup> One class of solutions to  
39 this problem involves more extensive brine post-treatment, possibilities for which have been

40 comprehensively reviewed elsewhere.<sup>8-10</sup> For instance, zero liquid discharge (ZLD) has been considered  
41 as a way to eliminate brine discharge. ZLD, however, presents high energy and capital costs,<sup>11</sup> largely as  
42 a result of the high concentrations which require energy intensive thermal desalination technologies.<sup>12-</sup>  
43 <sup>15</sup> The reuse of the brine to produce useful and valuable chemicals can be a more sustainable solution,  
44 although this approach is rarely applied due to the variety of impurities in the brine, leading to  
45 complex separation and purification needs.<sup>16</sup> Nevertheless, such a solution could limit harmful  
46 environmental impacts by reducing (or even eliminating) brine discharge; and this approach could cut  
47 plant costs or generate revenue, making fresh water more affordable.<sup>17</sup>

48 In this study, we focus on one example of brine chemical recovery: converting NaCl in brine to NaOH,  
49 commonly known as caustic or caustic soda, which can be re-used within the RO facility. NaOH is  
50 widely used to increase pH during pretreatment of seawater feed. At higher pH, aqueous boron  
51 compounds, toxic to human<sup>18</sup> and plant<sup>19,20</sup> health, exist primarily as charged borate species, which are  
52 better rejected by RO membranes.<sup>21,22</sup> Undesirable heavy metals and hardness, which can cause  
53 membrane scaling, can also be precipitated at high pH.<sup>23,24</sup> The use of caustic soda can hinder  
54 biofouling as well.<sup>25</sup> Further, caustic soda is used in the makeup of cleaning solutions for removing  
55 organic foulants and scales.<sup>26</sup> Converting RO brine to NaOH therefore can benefit both the  
56 environment and the financial bottom line by reducing brine discharge while simultaneously supplying  
57 in-plant chemical demand. Excess caustic soda produced might even be a profitable side-product of  
58 high-capacity seawater desalination plants: world annual consumption of NaOH is constantly growing,  
59 from 53 million tons in 2002 to over 65 million tons in 2015 and 82 million tons in 2020 (expected).<sup>27,28</sup>

60 The vast majority of NaOH used in RO plants today is manufactured by the chlor-alkali process, which  
61 accounts for 99.5% of caustic production worldwide.<sup>28</sup> The process electrolyzes near-saturated NaCl

62 brine, producing caustic soda as well as chlorine and hydrogen gas. Three main variants of the process  
63 exist, but the membrane variant, which uses a cation exchange membrane as the separator between  
64 catholyte and anolyte, is the most widely used and is considered the best available technology.<sup>29,30</sup>  
65 Membrane electrolyzers produce caustic soda of 32-35 wt% concentration, but the process requires a  
66 very pure feed brine of about 290-310 g/L NaCl concentration.<sup>31</sup> The major purity requirements are  
67 listed in the following:<sup>28,31-33</sup>

- 68 • Hardness ions ( $\text{Ca}^{2+} + \text{Mg}^{2+}$ ) < 0.02 ppm, as  $\text{Ca}^{2+}$  reduces current efficiency and both ions  
69 increase electrolyzer operating voltage;
- 70 • Free chlorine (chlorine and its active hydrolyzed forms, i.e. hypochlorite<sup>33</sup> < 0.1 ppm, as it  
71 damages ion-exchange resin (used for pretreatment) and reduces life of equipment and piping;
- 72 • Sulfate as  $\text{Na}_2\text{SO}_4$  < 4-8 g/L, as they reduce current efficiency of the electrolyzer.

73 These stringent purity requirements, particularly on hardness (< 0.02 ppm for  $\text{Ca}^{2+}$  and  $\text{Mg}^{2+}$ ),  
74 indicate that any RO-brine reused will require considerable treatment before being suitable for the  
75 chlor-alkali process.

76 Previous studies have suggested alternative approaches to treat seawater and/or its concentrated  
77 brine to obtain NaCl as intermediate product and ultimately to produce NaOH.<sup>34,35</sup> Others have  
78 focused more on the process of converting brine directly to a chlor-alkali feed without going through  
79 the intermediate stage of salt production.<sup>36,37</sup> Thiel et al.<sup>38</sup> provide a more detailed review of these and  
80 other technologies, along with thermodynamic benchmarks for each technology.

81 Beyond these past studies, no comprehensive model has been found in the literature that describes  
82 a full system to convert RO brine to caustic soda, including pretreatment and production. By combining  
83 the individual components, interrelations between components are to be considered and model

84 parameters are to be chosen and optimized in order to fit the whole system for caustic production  
85 directly from seawater. In this work, an Aspen Plus® model for the brine-to-caustic system, including  
86 purification and concentration components and membrane electrolysis cell, is constructed. Using the  
87 model, system productivity and the energy consumption of each component are determined.

88 In the section “Modeling methodology,” we introduce the overall modeling approach, system physics  
89 and the models employed for each component. In the section “System Parameterization, boundary  
90 Conditions,” we present and justify the values used to parameterize the components. In the section  
91 “Results and discussion,” we discuss the results from the model and the advantages of the process.  
92 Finally, the environmental implications of the present process are considered in the last section.

## 93 MODELING METHODOLOGY

94 In this section, we first introduce the modeling approaches and assumptions made. Thereafter we  
95 describe the process chain and its individual components to convert SWRO brine to caustic soda. To  
96 achieve the desired purification and concentration for the membrane electrolysis, essential  
97 pretreatment components are chosen based on their reliability and maturity.

## 98 MODELING APPROACH AND ASSUMPTIONS

99 Steady-state simulations in Aspen Plus are conducted with the focus on system-level performance of  
100 the conversion process. Details at the component-level (i.e., heat and mass transport phenomena,  
101 reaction kinetics) are not taken into consideration.

102 The ENRTL-RK model, which is implemented in Aspen, is applied to simulate the non-ideal  
103 thermodynamic behavior of brine and other relevant electrolyte streams. This model combines ENRTL  
104 (Electrolyte non-random two-liquid) model for the non-ideal electrolyte liquid phase and the Redlich-

105 Kwong (RK) equation of state for the gas phase. Originally developed by Chen<sup>39</sup>, the ENRTL model is a  
106 widely applied property model for process simulation of electrolyte systems with mixed solvent. Song  
107 and Chen<sup>40</sup> concluded that the ENRTL is preferred for process modeling applications, compared to  
108 other models (Pitzer, OLI MSE, UNIQUAC). In Aspen Plus, the improved ENRTL model from Song and  
109 Chen<sup>40</sup> is implemented.<sup>41</sup>

110 The following assumptions are made during the modeling:

- 111 • Seawater is considered as NaCl solution, contaminated with Ca<sup>2+</sup>, Mg<sup>2+</sup> (hardness ions),  
112 bromide (Br<sup>-</sup>) and sulfate ions (SO<sub>4</sub><sup>2-</sup>);
- 113 • Each stream is ideally mixed without temperature, pressure and concentration gradients;
- 114 • Chemical equilibria of aqueous phase reactions, including electrolyte dissociations and salt  
115 precipitations, are reached for every stream. These equilibria are predicted automatically by  
116 Aspen.

## 117 OVERALL PROCESS CHAIN

118 Figure 1 shows a block flow diagram with relevant components and streams: the SWRO brine is first  
119 purified by nanofiltration (NF) where most sulfate ions and a fraction of hardness ions (Ca<sup>2+</sup> and Mg<sup>2+</sup>)  
120 are removed. The NF permeate is concentrated by electrodialysis (ED), and further concentrated by  
121 evaporation or mechanical vapor compression up to NaCl saturation, as required by the electrolyzer.  
122 The remaining hardness ions in the brine are removed by chemical softening and ion exchange (IX).  
123 Finally, the sufficiently pure and concentrated brine is acidified and sent to the membrane electrolyzer  
124 to produce the products: NaOH, Cl<sub>2</sub>, and H<sub>2</sub>.

125 Nanofiltration (green box in Figure 1) is used to remove sulfate ions. High concentration of sulfates  
126 may cause  $\text{CaSO}_4$  fouling<sup>42</sup> in concentration units (ED, Evaporation). This explains why NF is put at the  
127 first step in the process chain. In addition, NF lowers Ca and Mg content of the brine,<sup>43,44</sup> reducing  
128 other fouling concerns.<sup>45</sup>

129 Electrodialysis (orange box in Figure 1) is chosen as the next step for a primary concentration. The  
130 employed NF-ED chain is also suggested by Garriga,<sup>36</sup> and ED is also recommended by Casas et. al.<sup>17</sup>  
131 The feed is split into two streams which are fed into a diluate and a concentrate channel. ED stack  
132 transports NaCl (and water) from the former to the latter. For industrial ED systems, the highest  
133 concentration achieved is around 200 g/kg (20 wt%).<sup>46</sup> The diluate outlet is set as 3.5 wt%. This outlet  
134 concentration corresponds to normal seawater and allows the ED diluate to be recycled as a feed into  
135 the RO plant.

136 Since the membrane cell requires nearly saturated brine, evaporation is used after ED as a final  
137 concentration step (pink box in Figure 1). The combination of ED and evaporation might be  
138 considerably more economic than evaporation alone, as suggested by Leitz.<sup>47</sup>

139 Mechanical vapor compression (MVC) is an alternative for evaporation. While the evaporator is  
140 simply heat-driven, MVC compresses the vapor produced by evaporation and powers the evaporator  
141 using this compressed vapor. With a preheating heat exchanger integrated, the only energy input is the  
142 mechanical work associated with the compressor.

143 After being concentrated to saturation, the brine goes through the chemical softening stage.  $\text{Na}_2\text{CO}_3$   
144 and NaOH are added to precipitate  $\text{Ca}^{2+}$  and  $\text{Mg}^{2+}$  ions as calcium and magnesium salts. These  
145 precipitates are then removed by filtration.

146 Chemical softening achieves a ppm-level hardness level which still does not meet the required purity  
147 for the electrolyzer cells.<sup>28</sup> Thus, a cation ion-exchange step is used as a final purification step to  
148 remove hardness down to ppb-level. The process chain of chemical softening, ion-exchange and  
149 electrolysis is a standard process in a typical membrane chlor-alkali plant.<sup>28</sup> Before entering the  
150 electrolyzer, the purified brine is acidified with HCl.

151 In the membrane electrolyzer, production of Cl<sub>2</sub>, H<sub>2</sub>, and caustic soda takes place, resulting in a  
152 depleted brine stream that typically contains up to 20 wt% NaCl. The depleted brine from the  
153 electrolysis cell must be dechlorinated (light blue component in Figure 1) before being discharged to  
154 the environment<sup>29</sup> or recycled.<sup>28</sup>

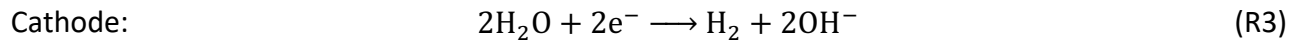
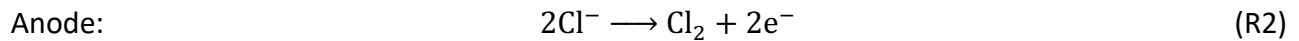
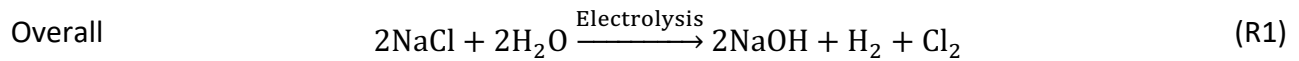
155 After dechlorination, the depleted brine is fed into a splitter and split into a purge stream (see  
156 “Purge stream” in Figure 1, mid left) and a recycled stream. The purge stream leaves the system. We  
157 define the ratio of the purged stream and the total stream fed to the splitter as the “purge ratio”. The  
158 role of the purge is to prevent impurities (primarily sulfate) from accumulating in the system (see  
159 section “Purge ratio”). This is also mentioned by the literature<sup>28</sup> as one of the methods to control  
160 sulfate. Other possible sulfate removal/controlling methods would be an additional NF stage or the  
161 usage of barium salts in chemical softening. However, the former leads to NaCl depletion<sup>48</sup> and the  
162 latter involves the usage of expensive and toxic barium salts.<sup>29</sup> Thus, both options are not favored  
163 here.

164 The recycle stream has a brine concentration of around 20 wt%<sup>28</sup> and does not require the primary  
165 concentration of ED, so it is fed back to the evaporation/MVC component.

166

167 MODELING OF MEMBRANE ELECTROLYZER

168 The ion-exchange membrane in the electrolyzer separates the electrolysis cell into anode and  
169 cathode chambers. The overall reaction is (R1). On the anode, chloride is oxidized to chlorine via (R2).  
170 On the cathode, water is reduced to hydrogen and hydroxide ions according to (R3).



171

172 A typical membrane electrolysis cell is illustrated in Figure 2. On the anode (blue), chloride is oxidized  
173 to chlorine gas, part of which is dissolved in the anolyte.<sup>49</sup> The side reaction is water oxidation,  
174 producing oxygen. Extents of both reactions depend on the process chlorine efficiency  $\xi^P$  and the  
175 anode current efficiency  $\xi$ .<sup>50</sup> The definition of these efficiencies is elaborated in the Supplementary  
176 Information (SI) section “Anode chamber.” On the cathode (red), water is reduced to hydrogen,  
177 producing hydroxide ions. Part of them migrates back to the anolyte, reducing the sodium transport by  
178 a factor of  $\eta$ , the cathode current efficiency (see SI section “Cathode chamber and membrane  
179 transport”). Typically, the anode side brine has depletion of NaCl from 26 wt% to 20 wt% and the feed  
180 caustic concentrates NaCl from 30 wt% to 32 wt%. Some of the 32 wt% caustic is taken as product; the  
181 rest is slightly diluted to 30 wt% using deionized water and recirculated.

182 The detailed Aspen modeling for the electrolyzer is elaborated in the SI section “Modeling of  
183 membrane electrolyzer in Aspen Plus”. Additionally, model validation is conducted against a set of  
184 reference plant data in the literature<sup>28</sup>, which is described in SI section “Validation of membrane  
185 electrolyzer model”. The agreement with literature values shows the accuracy of the electrolyzer  
186 model and the applied thermodynamic property model.

187

188

## 189 ENERGY CONSUMPTION

190 The energy consumption of the electrolyzer can be calculated as follows:

$$\dot{W}_{\text{cell}} = U_{\text{cell}} \cdot I_{\text{cell}} = U_{\text{cell}} \cdot F \cdot \frac{\Delta \dot{n}_{\text{NaOH}}}{\eta} \quad (1)$$

191 The cell voltage,  $U_{\text{cell}}$ , is assumed constant at 3.2 V, a value taken from reference plant data given in  
192 the literature.<sup>28</sup> It shall be noted that in real cells, the cell voltage increases with increasing current due  
193 to the ohmic loss in the cell and the over-voltage on both electrodes.<sup>28</sup>

## 194 MODELING OF OTHER COMPONENTS

195 The modeling of other components used in the process chain, including brine acidifier, ion-  
196 exchanger, chemical softening, evaporator, MVC, electrodialysis, nanofiltration, dechlorination and  
197 brine purge, are elaborated in the Supplementary Information (SI) section “Modeling of other  
198 components in Aspen Plus”.

## 199 SYSTEM PARAMETERIZATION, BOUNDARY CONDITIONS

200 In this section, the feed brine composition is given as a boundary condition of the model. Parameter  
201 values used in each individual component of the Aspen modeling are listed in Table 1. More details  
202 including parameters of individual components are given in Table S6 of the SI.

203

## 204 RESULTS AND DISCUSSION

205 This section introduces the results obtained by this study. First, we evaluate the energy consumption  
206 and thermodynamic efficiency of each component and give some suggestions for system  
207 improvement. Next, we show the dependency of system performance on two important process  
208 parameters based on a sensitivity study and justify our chosen parameter values. Then, we use the  
209 obtained chemical dosage requirements and energy consumption numbers to estimate the operating  
210 expense (OPEX) of the system and compare it with standard chlor-alkali. Last, we discuss the  
211 advantages, best-use examples, and challenges of the proposed process.

## 212 OVERALL PRODUCTIVITY

213 From 17.5 t/h brine feed to the process, the membrane electrolyzer produces 208.4 kg/h of 32 wt%  
214 NaOH (66.7 kg/h as equivalent dry product). While 1.9 kg/h of it (around 3 %) should be used internally  
215 for the chemical softening and ion-exchange components, the real caustic output amounts to 64.8 kg/h  
216 (as dry). A summary of mass flows at each stage can be found in Table S7 of the SI. The model is  
217 scalable with mass, thus allowing its application to a different NaOH production rate.

## 218 ENERGY CONSUMPTION AND SECOND LAW EFFICIENCY OF COMPONENTS

219 In industry, energy costs dominate the chlor-alkali process and most high-concentration processes.  
220 For this process chain, the energy consumption, least work, and second law efficiencies of various  
221 components are illustrated in Figure 3.

222 Notably, two options are given for the brine saturation component: the evaporator or the MVC. The  
223 evaporator consumes 190.8 kW heat (2.94 kWh/kg NaOH) whereas the MVC component consumes  
224 15.75 kW electricity (0.24 kWh/kg NaOH). Regardless of this concentration component, the rest of the  
225 system (NF, ED, electrolyzer) consumes about 189.9 kW (2.93 kWh/kg NaOH) electricity.

226

227 The second law efficiency, given by Equation (2), is a quantitative measure for the thermodynamic  
228 efficiency of a given process. Equation (2) can be applied for processes including both work  $\dot{W}$  and  
229 heat input  $\dot{Q}$ :<sup>56,57</sup>

$$\eta_{II} = \frac{\dot{W}_{\text{least}}}{\dot{W} + \left(1 - \frac{T_{\infty}}{T_Q}\right) \cdot \dot{Q}} \quad (2)$$

230 where  $T_{\infty}$  is the ambient temperature, and  $T_Q$  is the temperature of the heat source (both in K). In the  
231 evaporator, we assume the use of 1.2 bar saturated steam (123.5 °C) as the heat source, which is  
232 reasonable condition for industrial waste steam.  $\dot{W}_{\text{least}}$  is the thermodynamic least work. Its  
233 calculation is elaborated in the SI (equation S-10).

234

235 The chlor-alkali electrolysis consumes the most energy in the process. However, it shows good  
236 thermodynamic efficiency (68.2 %), limiting potential improvements. Irreversibilities are mainly caused  
237 by limited current efficiency and voltage losses (due to overvoltages on the electrodes and the ohmic  
238 losses in the solution, the membrane, and the metal hardware).<sup>28</sup> Nevertheless, this efficiency assumes  
239 that  $\text{Cl}_2$  and  $\text{H}_2$  are desired products beside NaOH. If, instead, NaOH is the only product of interest and  
240 HCl is produced as side product (by combusting  $\text{H}_2$  and  $\text{Cl}_2$ ), the chlor-alkali electrolysis efficiency  
241 decreases to 39.4 % when no energy is recovered from the formation of HCl.

242 The evaporator, as the second highest energy consumer in the process, shows a poor second law  
243 efficiency (3.5 %). Better use of the steam produced (i.e., to preheat before the electrolyzer) would  
244 increase the efficiency of this component significantly.

245 Overall, improvement of the energy efficiency of brine concentration components represents the  
246 most feasible route to significant energy savings. Processes not requiring as much brine concentration  
247 as electrolysis could yield very significant energy savings.<sup>38,58</sup>

248

## 249 SENSITIVITY STUDIES

250 Modeling of the brine-to-caustic process in Aspen allows the variation of certain parameters to  
251 reveal their impact on the system performance. The key parameters from the process chain chosen  
252 here are the anolyte outlet concentration of the electrolyzer (depleted brine in Figure 2) and the  
253 “purge ratio” of the recycling brine (Figure 1, after the dechlorination block). During the sensitivity  
254 study, all system parameter values (see Table 1) are kept constant except for the varied parameter.

255

### 256 ANOLYTE OUTLET CONCENTRATION

257 System performance is heavily influenced by the concentrations of streams related to the  
258 recirculation of depleted brine from the electrolyzer back into the concentration stages. A lower  
259 anolyte outlet concentration corresponds to a higher conversion of NaCl to NaOH in the electrolyzer  
260 cell, and therefore high caustic productivity. However, this requires that the recycled brine must be  
261 concentrated more, resulting in a higher absolute energy consumption in the evaporator/MVC  
262 component. This high absolute energy consumption is offset by the higher caustic productivity in the  
263 electrolyzer. Overall, the electrolyzer productivity wins this competition: the specific energy  
264 consumption, normalized by the caustic production is lower at low anolyte outlet concentrations, as  
265 shown in Figure 4.

266 It is evident from Figure 4 that by lowering the anolyte concentration from 22 wt% to 18 wt%, the  
267 evaporator/ MVC component is consuming about 10% less specific energy. Technically, this means a  
268 high applied current and a great depletion of the feed NaCl in the electrolysis cell are beneficial for the  
269 whole brine-to-caustic process in terms of productivity and energy consumption. However, as shown in  
270 Figure 4, a lower limit exists at 18.2 wt% (200 g/L), below which a stable operation of the membrane  
271 electrolyzer cell is no longer feasible.<sup>28</sup>

272 Based on the results of this sensitivity study, we chose 19 wt% as the anolyte outlet concentration of  
273 the electrolyzer (Table 1) which allows high system productivity at low specific energy consumption  
274 while avoiding the danger of unstable operation by providing a safe margin between the operation  
275 point and the lower limit.

276

277

278 PURGE RATIO

279 Purging refers to removing a fraction of the depleted brine from the system using a simple splitter,  
280 allowing only a remaining fraction to reenter the process (see Figure 1). This prevents impurities,  
281 primarily sulfate, from accumulating in the system. To limit the sulfate concentration in the membrane  
282 cell under the allowable tolerance, a minimal purge fraction is needed, which is determined based on  
283 the sensitivity study here.

284 The purge ratio (removed stream by the splitter divided by total stream entering the splitter) is  
285 varied from 0.2 to 1. The electrolyzer feed mass flow as well as its sulfate content with respect to the  
286 purge ratio is shown in Figure 5.

287 Figure 5 shows that the mass flow into the electrolyzer is decreasing with increasing purge ratio  
288 (horizontal axis). As shown, less purge and more recycling leads to higher system productivity. The  
289 recycling, however, is limited by the sulfate accumulation in the system. The impurities bromine and  
290 chlorate also accumulate, but at lower concentrations and further below tolerances than sulfate. As  
291 seen in Figure 5, a purge ratio between 0.3 and around 0.45 risks adverse effects (yellow zone) by high  
292 sulfate concentration (red line), and a ratio below 0.3 risks extreme impact by sulfate (red zone).

293 Based on this sensitivity study, a 0.5 purge ratio is selected for the system-level process,  
294 corresponding to a 1:1 ratio of recycle and purge streams. According to Figure 5, this purge ensures an  
295 electrolyzer feed sulfate concentration of about 3 g/L  $\text{Na}_2\text{SO}_4$  (in the green zone) which maximizes cell  
296 performance while preventing possible adverse effects of sulfate accumulation.

## 297 OPERATION COSTS

298 With the energy consumption and chemical dosage obtained from the process model, the  
299 operational cost (OPEX) of the proposed system can be estimated. The calculations are summarized in  
300 Table 2.

301  
302 Evidently, energy costs are dominant in the OPEX of the whole process. The membrane electrolyzer,  
303 as the primary energy consumer, contributes almost two thirds of the total operation costs.  
304 Concentration components ED, evaporator or MVC also has significant energy costs. Nevertheless, if  
305 the desalination plant is co-located with a power-plant (this is not uncommon), low grade heat could  
306 potentially be diverted to help lower the concentration cost.

307 Besides operating costs, the capital expenditure (CAPEX) also plays a dominant role in such a long-  
308 chain process. However, its estimation is highly site-specific, depending on several economic and other

309 factors, and thus having very limited accuracy in a general case. We will not further focus on it but  
310 point out that it could be a direction for further studies.

311

## 312 COMPARISON OF THE PROCESS CHAIN WITH SIMILAR PROCESSES

313 In this section, our model for the process chain is compared against other existing models and the  
314 improvements and suggestions for future design are noted.

### 315 COMPARISON WITH STANDARD CHLOR-ALKALI

316 The major difference of the proposed process from the standard chlor-alkali industry lies in the feed  
317 stream. The feedstock in chlor-alkali industry is usually highly pure rock salt which requires no  
318 concentration step and fewer purification steps. As shown in Table 2, the pretreatment steps (NF, ED,  
319 MVC, chemical softening) in the brine-to-caustic process would cost around 0.0588 \$ per kilogram  
320 caustic soda produced. If caustic soda were produced in excess of the brine-to-caustic needed  
321 internally at the RO plant (i.e., to generate extra revenue), this pretreatment cost should be compared  
322 with local rock salts (including the availability of rock salts locally, and the cost and quality of available  
323 salts) to decide whether it is economically feasible to produce excess saturated NaCl solution from RO  
324 brine.

325

### 326 COMPARISON WITH MELIAN-MARTEL<sup>37</sup>

327 In Melian-Martel's model of caustic production from RO brine, instead of controlling the sulfate  
328 concentration in the system by purging, barium is used to precipitate sulfate salts. Melian-Martel et al.

329 proposed the following process: Softening-MEE-IX-Electrolysis, where MEE is multi-effect-evaporation.  
330 The depleted brine from the electrolyzer is recycled after a dechlorination process. Additionally, they  
331 have calculated flows and concentrations in each stage.

332 While the final objective of their study is similar to ours, our process has the following differences/  
333 improvements:

- 334 • Removal of sulfate: In our process, nanofiltration is used to reduce sulfate along with a brine  
335 purge, instead of using toxic and expensive barium salts. The sulfate concentration does not  
336 need to be lowered to the level of chemical precipitation as membrane cells are somewhat  
337 tolerant (purity requirements given in the section “Modeling details”).
- 338 • Method of concentration: Melian-Martel used multi-effect evaporation (MEE) as a single-step  
339 concentration while we used ED as primary step and evaporation/MVC as final step. This  
340 saves energy.
- 341 • NaCl concentration: Melian-Martel’s system concentrates the NaCl to 36 wt% in the MEE, and  
342 then dilutes it to 30.6 wt% for input to the membrane electrolyzer. In our system, maximal  
343 brine concentration is between 26 and 27 wt%. We suggest that high NaCl over-saturation (>  
344 27 wt%) should be avoided as the precipitation of NaCl crystals may cause scaling in  
345 evaporators and pipes.

346 Overall, our process is technically more feasible due to the absence of oversaturated brines. Brine  
347 purging to remove sulfate is also easy to operate and reduces chemical treatment costs.

#### 348 COMPARISON WITH GARRIGA<sup>36</sup>

349 The primary difference between the process chain suggested by Garriga and the present work is the  
350 addition of brine recycling. Garriga’s process chain is NF-ED-Saturation-Softening-IX-Electrolysis.

351 Saturation is achieved by adding solid NaCl, as in the chlor-alkali industry. However, as salt is not  
352 presumed to be available as feedstock, the present process uses evaporation/MVC instead. Our  
353 process also has higher productivity and lower effluent volume due to the recycling of depleted brine.

#### 354 ADVANTAGES, BEST-USE CASE, AND CHALLENGE OF THE PROCESS

355 Overall, the brine-to-caustic process investigated has the following advantages:

- 356 • Reduction of effluent from the RO facility:

357 Overall, this process can reduce up to 29% of the RO facility effluent. The effluents of the  
358 process (see Figure 1) are the NF retentate (rate of 12.20 t/h) and the brine purge of (0.26 t/h)  
359 which in Figure 1 are the green box right next to RO bring inlet and the green arrow coming out  
360 of the teal box of dechlorination. The effluents have a higher concentration than the RO brine  
361 and can possibly be further concentrated in zero-liquid discharge processes, such as  
362 evaporation ponds.

- 363 • Reusing ED diluate:

364 The ED step not only concentrates the brine, but also can improve the production of pure water  
365 thus reducing pure water costs as well. The ED diluate can be fed back to SWRO for increased  
366 recovery, since the diluate's concentration of 3.5 wt% matches regular seawater. As this stream  
367 amounts for 26.2% of the RO brine, the actual water recovery of a regular RO plant (50%) would  
368 increase to 57.5%. Additionally, since this recycle stream comes from the RO brine, it does not  
369 require the costly extra pretreatment in the SWRO system which is necessary for fresh  
370 seawater.

- 371 • Avoiding of concentration-dilution cycle:

372 The proposed process avoids the steps of NaCl and NaOH concentration, transportation and  
373 dilution that are standard in chlor-alkali industry and desalination plants.

374 In standard chlor-alkali systems, solid salt is used as the feedstock and mostly originates  
375 from energy intensive evaporation and crystallization of an NaCl solution. Yet no energy is  
376 recovered when the salt is transported to a chlor-alkali facility and dissolved, resulting a loss of  
377 about 2.58 kWh heat per kg NaOH produced.

378 In RO plants, 50 wt% NaOH solution is typically obtained from chlor-alkali facilities and  
379 diluted for internal use. However, the 50 wt% solution is produced by evaporating the 30-35  
380 wt% caustic soda from the electrolyzer.<sup>28</sup> This fraction of energy input (about 0.70 kWh heat/kg  
381 NaOH) is wasted by dilution.

382 • Potential revenue from side products:

383 The side products of the chlor-alkali process, H<sub>2</sub> and Cl<sub>2</sub>, can generate substantial revenue. First,  
384 for every kilogram of caustic soda produced, 27.6 grams of hydrogen with a heat value of 0.92  
385 kWh is co-produced. This heat could be directly applied in the evaporation step. Second, a  
386 relatively large amount of chlorine is produced, namely 0.87 kg per kg NaOH. Assuming a price  
387 of 250 \$/t<sup>61</sup> for chlorine, the potential revenue amounts to 0.22 \$/kg NaOH, nearly covering the  
388 operation costs listed in Table 2. It is crucial to mention, however, that the chlorine obtained  
389 through this process is a crude product (contains O<sub>2</sub>, H<sub>2</sub>O, possibly N<sub>2</sub> and CO<sub>2</sub>) that can either  
390 be sold for a low price or has to be purified and liquefied yielding additional operation and  
391 capital costs.

392                    Additionally, besides H<sub>2</sub> and Cl<sub>2</sub>, it is also possible to produce more valuable side  
393                    products on site, such as sodium hypochlorite, a typical bleaching chemical that is produced  
394                    from NaOH and Cl<sub>2</sub>.

- 395                    • Reduction of transportation costs:

396                    The onsite production eliminates the transportation costs of NaOH for internal usage in SWRO  
397                    plants.

398                    Additionally, as water is produced in RO facility as well as in the evaporator/MVC  
399                    component of the brine-to-caustic system, the transportation costs of deionized water for the  
400                    membrane electrolyzer (see Figure 1) can be saved.

401                    The best-use case of the proposed brine-to-caustic process would be an SWRO desalination plant,  
402                    satisfying some of the following points:

- 403                    • Locations with scarce or expensive rock salt resources, corresponding to high price for standard  
404                    chlor-alkali feedstock, and therefore making the brine-to-caustic process economically feasible  
405                    not only for internal usage, but also for producing extra NaOH and Cl<sub>2</sub> for revenue.
- 406                    • Remote desalination plants which are far from the nearest chlor-alkali facility, causing high  
407                    transportation costs.
- 408                    • High restrictions of boron content in the freshwater leading to high internal caustic usage.
- 409                    • Limitations for RO brine discharge or legal benefits for low-impact discharge methods.
- 410                    • Possible co-existing power plants that can supply waste heat for concentration processes.
- 411                    • Possible co-existing chemical plants that can utilize the produced chlorine and excess NaOH.

412

413 Nevertheless, several challenges related to the process remain, for example the required know-how  
414 for each component in such an integrated process, as well as operation and control issues, especially  
415 during start-up and shut-down.

## 416 ENVIRONMENTAL IMPLICATIONS

417 The energy consumption and environmental impact of desalinated water production has become a  
418 major concern, especially due to the relative energy demands and required disposal of concentrated  
419 brine. The brine is usually discharged as wastewater, which can create a local imbalance in the ocean's  
420 salinity with negative impacts on marine ecosystems. Additionally, the treatment of water requires the  
421 use of caustic soda, of which the production and transportation contributes indirectly to the energy  
422 consumption of water production.<sup>62</sup>

423 In this study, a recovery process for creating caustic soda from desalination brine has been  
424 developed focusing on purification requirements and energy efficiency.

425 The present research not only develops a feasible process to produce caustic soda on-site at  
426 seawater desalination plants, but also explores the productivity, the energy use of the overall process,  
427 and the thermodynamic performance of the individual components. This process, as proposed at  
428 small-scale, can produce hundreds of metric tons of NaOH (a dry equivalent) per year, an amount that  
429 would fulfill the caustic soda needs of a typical, large-scale SWRO plant.<sup>38</sup> Moreover, if our NaOH  
430 recovery process was used on all the brine from a large-scale SWRO plant (about 10,000 kt/year), over  
431 35,000 t caustic could be produced for commercial sale. The excess caustic production could be  
432 economically attractive, especially for desalination plants in remote locations, or with expensive local  
433 salt resources. Additionally, desalination plants using this process for the brine could increase typical  
434 water recovery from 50% to around 58%, reduce brine disposal volumes by 29%, save on pretreatment

435 costs of feed water, and thus lower the normalized cost of freshwater. Furthermore, our process has a  
436 potential to reduce transportation, disposal costs, and emissions involved in brine disposal in other  
437 desalination applications that require zero liquid discharge.

## 438 ACKNOWLEDGEMENTS

439 The authors of this work gratefully acknowledge sponsorship by Cadagua, a Ferrovial subsidiary,  
440 through the MIT Energy Initiative. Aspen Plus from AspenTech, Inc. is used in this research. The authors  
441 also wish to thank Kishor G. Nayar for his suggestions on electrodialysis as well as Alicia Gómez  
442 González and Luis Alberto Letona Cabrera at Cadagua for providing important input parameters and  
443 giving practical insights.

## 444 CONTENTS OF SUPPORTING INFORMATION

- 445 • Brief introduction of modeling in Aspen Plus
- 446 • Modeling details of the membrane electrolyzer, validation and parametric study of the model
- 447 • Modeling details of the pre- and post-treatment components in the brine-to-caustic process  
448 chain
- 449 • Summary of mass flow, temperature and concentration at each stage of the process
- 450 • Brief introduction of least work analysis

## 451 NOMENCLATURE

### 452 Roman Symbols

$f$	-	Water transport number
$F$	C/mol	Faraday's constant (96,485 C/mol)
$I$	A	Electric current

453		$\dot{n}$	kmol/h	Molar flow
		$\dot{Q}$	kW	Heat flow
		$T$	°C	Temperature
		$U$	V	Voltage
		$\dot{W}$	kW	Work flow

454 Greek Symbols

	$\eta$	-	Cathode current efficiency
	$\eta_{ED}$	-	Current utilization factor in electrodialysis
	$\eta_{II}$	-	Second law efficiency
	$\xi$	-	Chlorine current (anode current) efficiency
	$\xi^P$	-	Process chlorine efficiency

455 Subscripts

	$\infty$	Ambient
	cell	Electrolyzer cell
	least	Least (work)
	$Q$	Heat source

457 Abbreviations

	ED	Electrodialysis
	ENRTL	Electrolyte- Non-random-two-liquid
	IX	Ion-exchange
	MEE	Multi-effect evaporation
	MVC	Mechanical vapor compression
	NF	Nanofiltration
	ppb	Parts per billion ( $\mu\text{g}/\text{kg}$ )
	ppm	Parts per million ( $\text{mg}/\text{kg}$ )
	RK	Redlich-Kwong (equation of state)
	RO	Reverse osmosis
	SWRO	Seawater reverse osmosis
	ZDL	Zero liquid discharge

459  
460

461 REFERENCES

- 462 (1) Khawaji, D.; Kutubkhanah, I. K.; Wie, J.-M. Advances in seawater desalination technologies.  
463 *Desalination* **2008**, 221 (1-3), 47–69.
- 464  
465 (2) Ghaffour, N.; Missimer, T. M.; Amy, G. L. Technical review and evaluation of the economics  
466 of water desalination: current and future challenges for better water supply sustainability.  
467 *Desalination* **2013**, 309, 197–207.

468  
469  
470  
471  
472  
473  
474  
475  
476  
477  
478  
479  
480  
481  
482  
483  
484  
485  
486  
487  
488  
489  
490  
491  
492  
493  
494  
495  
496  
497  
498  
499  
500  
501  
502  
503  
504  
505  
506  
507  
508  
509

- (3) Semiat, R. Energy issues in desalination processes. *Environ. Sci. Technol.* **2008**, *42* (22), 8193–8201.
- (4) Warsinger, D. M.; Tow, E. W.; Nayar, K. G.; Maswadeh, L. A.; Lienhard, J. H. Energy efficiency of batch and semi-batch (CCRO) reverse osmosis desalination. *Water Res.* **2016**, *106*, 272–282.
- (5) Adham, S.; Burbano, A.; Chiu, K.; Kumar, M. Development of a NF/RO knowledge base, California Energy Commission. *Public Interest Energy Research Program Report*, **2005**.
- (6) Roberts, D. A.; Johnston E. L.; Knott, N. A. Impacts of desalination plant discharges on the marine environment: A critical review of published studies. *Water Res.* **2010**, *44*, 5117–5228.
- (7) Lattemann, S.; Höpner, T. Environmental impact and impact assessment of seawater desalination. *Desalination* **2008**, *220* (1-3), 1–15.
- (8) Pérez-González, A.; Urtiaga, A. M.; Ibáñez, R.; Ortiz, I. State of the art and review on the treatment technologies of water reverse osmosis concentrates. *Water Res.* **2012**, *46*, 267–283.
- (9) Rodríguez-DeLaNuez, F.; Franquiz-Suárez, N.; Santiago, D. E.; Veza, J. M.; Sathwani, J. J. Reuse and minimization of desalination brines: a review of alternatives. *Desalin. Water Treat.* **2012**, *39*, 137–148.
- (10) Xu, P.; Cath, T. Y.; Robertson, A. P.; Reinhard, M.; Leckie, J. O.; Drewes, J. E. Critical review of desalination concentrate management, treatment and beneficial use. *Environ. Eng. Sci.* **2013**, *30* (8), 502–514.
- (11) Tong, T.; Elimelech, M. The global rise of zero liquid discharge for wastewater management: drivers, technologies, and future directions. *Environ. Sci. Technol.* **2016**, *50* (13), 6846–6855.
- (12) Warsinger, D. E.; Swaminathan, J.; Lienhard, J. H. Effect of module inclination angle on air gap membrane distillation. *Proceedings of the 15th International Heat Transfer Conference* **2014**.
- (13) Rezaei, M.; Warsinger, D. M.; Lienhard, J. H.; Samhaber, W. M. Wetting prevention in membrane distillation through superhydrophobicity and recharging an air layer on the membrane surface. *J. Membrane Sci.* **2017**, *530*, 42–52.

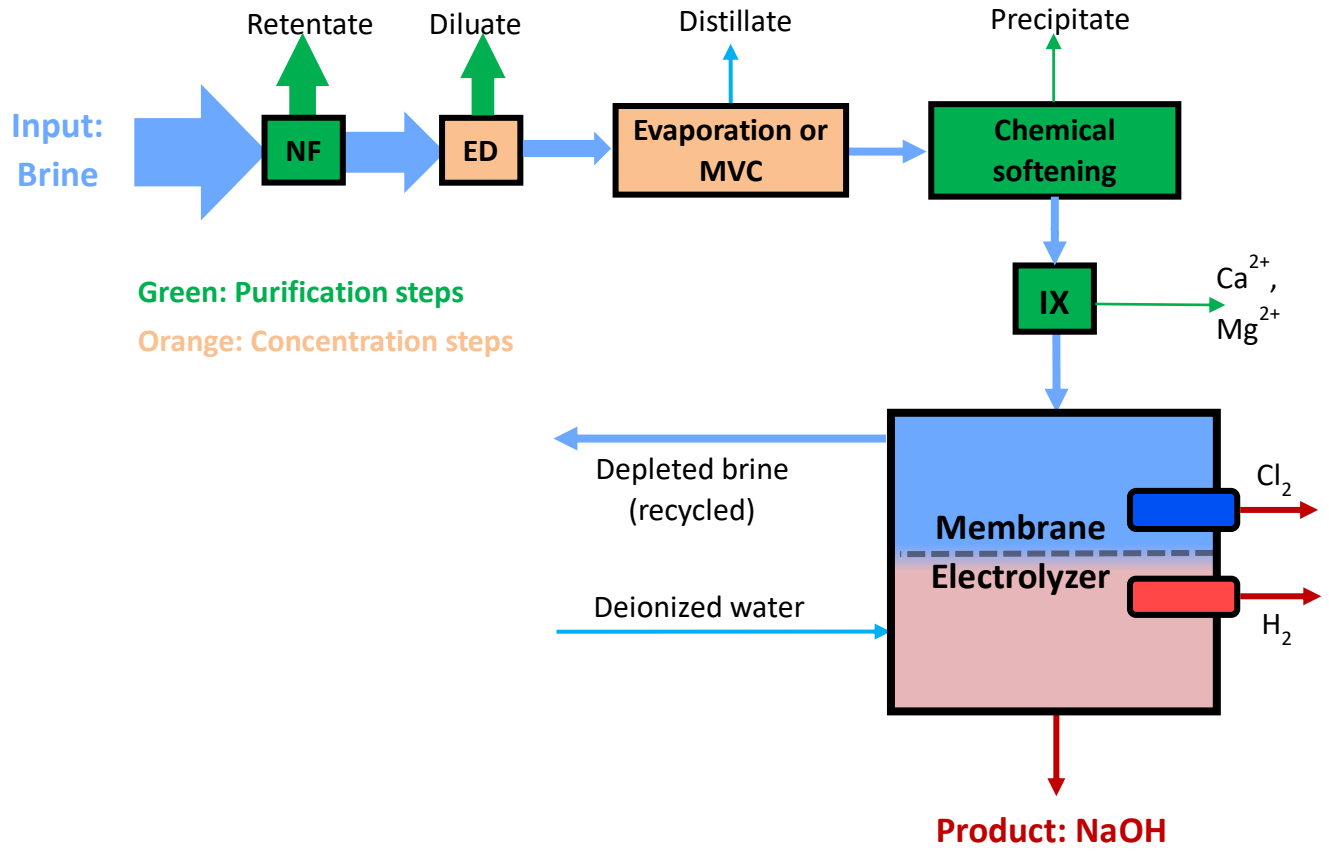
- 510 (14) Warsinger, D. M.; Swaminathan, J.; Morales, L. L.; Lienhard, J. H. Comprehensive  
511 condensation flow regimes in air gap membrane distillation: visualization and energy  
512 efficiency. *J. Membrane Sci.* **2018** (in press) <https://doi.org/10.1016/j.memsci.2018.03.053>.  
513
- 514 (15) Warsinger, D. E.; Swaminathan, J.; Maswadeh, L. A., Lienhard, J. H. Superhydrophobic  
515 condenser surfaces for air gap membrane distillation. *J. Membrane Sci.* **2015**, *492*, 578–587.  
516
- 517 (16) Van der Bruggen, B.; Lejon, L.; Vandecasteele, C. Reuse, treatment, and discharge of the  
518 concentrate of pressure-driven membrane processes. *Environ. Sci. Technol.* **2003**, *37*  
519 (17), 3733–3738.  
520
- 521 (17) Casas, S.; Aladjem, C.; Cortina, J.; Larrotcha, E.; Cremades, L. Seawater reverse osmosis  
522 brines as a new salt source for the chlor-alkali industry: integration of NaCl concentration by  
523 electrodialysis. *Solvent Extr. Ion Exc.* **2012**, *30* (4), 322–332.  
524
- 525 (18) Murray, F. J. A human health risk assessment of boron (boric acid and borax) in drinking  
526 water. *Regul. Toxicol. Pharm.* **1995**, *22* (3), 221–230.  
527
- 528 (19) Lenntech BV, Desalination Post-treatment: Boron Removal Process.  
529 [http://www.lenntech.com/processes/desalination/post-treatment/post-treatments/boron-](http://www.lenntech.com/processes/desalination/post-treatment/post-treatments/boron-removal.htm)  
530 [removal.htm](http://www.lenntech.com/processes/desalination/post-treatment/post-treatments/boron-removal.htm) (Revised on 2017.07.04).  
531
- 532 (20) Koç, C.; Effects on environment and agriculture of geothermal wastewater and boron  
533 pollution in Great Menderes Basin. *Environ. Monit. Assess.* **2007**, *125* (1), 377–388.  
534
- 535 (21) Magara, Y.; Kawasaki, M.; Sekino, M.; Yamamura, H. Development of reverse osmosis  
536 membrane seawater desalination in Japan. *Water Sci. Technol.* **2000**, *41* (10-11), 1–8.  
537
- 538 (22) Chua, K.; Hawlader, M.; Malek, A. Pretreatment of seawater: results of pilot trials in  
539 Singapore. *Desalination* **2003**, *159* (3), 225–243.  
540
- 541 (23) Rahardianto, A.; Gao, J.; Gabelich, C. J.; Williams, M. D.; Cohen, Y. High recovery membrane  
542 desalting of low-salinity brackish water: integration of accelerated precipitation softening  
543 with membrane RO. *J. Membrane Sci.* **2007**, *289* (1), 123–137.  
544
- 545 (24) Valavala, R.; Sohn, J.; Han, J.; Her, N.; Yoon, Y. Pretreatment in reverse osmosis seawater  
546 desalination: a short review. *Environmental Engineering Research* **2011**, *16* (4), 205–212.  
547
- 548 (25) Lin, H.-W.; Rabaey, K.; Keller, J.; Yuan, Z.; Pikaar, I. Scaling-free electrochemical production  
549 of caustic and oxygen for sulfide control in sewers. *Environ. Sci. Technol.* **2015**, *49* (19),  
550 11395–11402.  
551
- 552 (26) Nitto Hydranautics, Foulants and cleaning procedures for composite polyamide RO  
553 membrane elements. Technical Report Nitto Hydranautics, 2011.

- 554  
555 (27) *Global consumption of caustic soda to reach 82-MT by 2020.*  
556 <https://www.oceanicpharmachem.com/global-consumption-of-caustic-soda-to-reach-82->  
557 [mt-by-2020](https://www.oceanicpharmachem.com/global-consumption-of-caustic-soda-to-reach-82-) (Revised on 2017.07.04).  
558
- 559 (28) O'Brien, T. F.; Bommaraju, T. V.; Hine, F. *Handbook of Chlor-Alkali Technology*. Springer,  
560 2005.  
561
- 562 (29) Brinkmann, T.; Santonja, G. G.; Schorcht, F.; Roudier, S.; Sancho, L. D. Best available  
563 techniques (BAT) reference document for the production of chlor-alkali. Technical Report  
564 European Commission, Joint Research Centre, 2014.  
565
- 566 (30) EuroChlor, Chlorine industry review 2014-2015: Maintaining momentum in uncertain times.  
567 Technical Report EuroChlor.  
568
- 569 (31) Bommaraju, T. V.; Lüke, B.; O'Brien, T. F.; Blackburn, M. C. Chlorine. *Kirk-Othmer*  
570 *encyclopedia of chemical technology*, 2004.  
571
- 572 (32) Schmittinger, P.; Florkiewicz, T.; Curlin, L. C.; Lüke, B.; Scannell, R.; Navin, T.; Zelfel, E.;  
573 Bartsch, R. Chlorine. *Ullmann's Encyclopedia of Industrial Chemistry*, 1986  
574
- 575 (33) O'Brien, T. Dechlorination of brines for membrane cell operation. In *Modern Chlor-Alkali*  
576 *Technology*, pp. 251–270, Springer, 1990.  
577
- 578 (34) Kobuchi, Y.; Terada, Y., Tani, Y. The first salt plant in the middle east using electrodialysis  
579 and ion exchange membranes. In *Sixth International Symposium on Salt II 1983* (pp. 541–  
580 555).  
581
- 582 (35) Al-Mutaz, I. S.; Wagialla, K. M. Techno-economic feasibility of extracting minerals from  
583 desalination brines. *Desalination* **1988**, *69* (3), 297–307.  
584
- 585 (36) Garriga, S. C. Valorization of brines in the chlor-alkali industry. Integration of precipitation  
586 and membrane processes. PhD thesis, Universitat Politècnica de Catalunya, 2011.  
587
- 588 (37) Melián-Martel, N.; Sathwani, J. J.; Báez, S. O. P. Saline waste disposal reuse for desalination  
589 plants for the chlor-alkali industry: The particular case of pozo izquierdo SWRO desalination  
590 plant. *Desalination* **2011**, *281*, 35–41.  
591
- 592 (38) Thiel, G. P.; Kumar, A.; Gómez-González, A.; Lienhard, J. H. Utilization of desalination brine  
593 for sodium hydroxide production: Technologies, engineering principles, recovery limits and  
594 future directions. *ACS Sustain. Chem. Eng.* **2017**, *5* (12), 11147–11162.  
595
- 596 (39) Chen, C.-C.; Evans, L. B. A local composition model for the excess Gibbs energy of aqueous  
597 electrolyte systems. *AIChE J.* **1986**, *32* (3), 444–454.

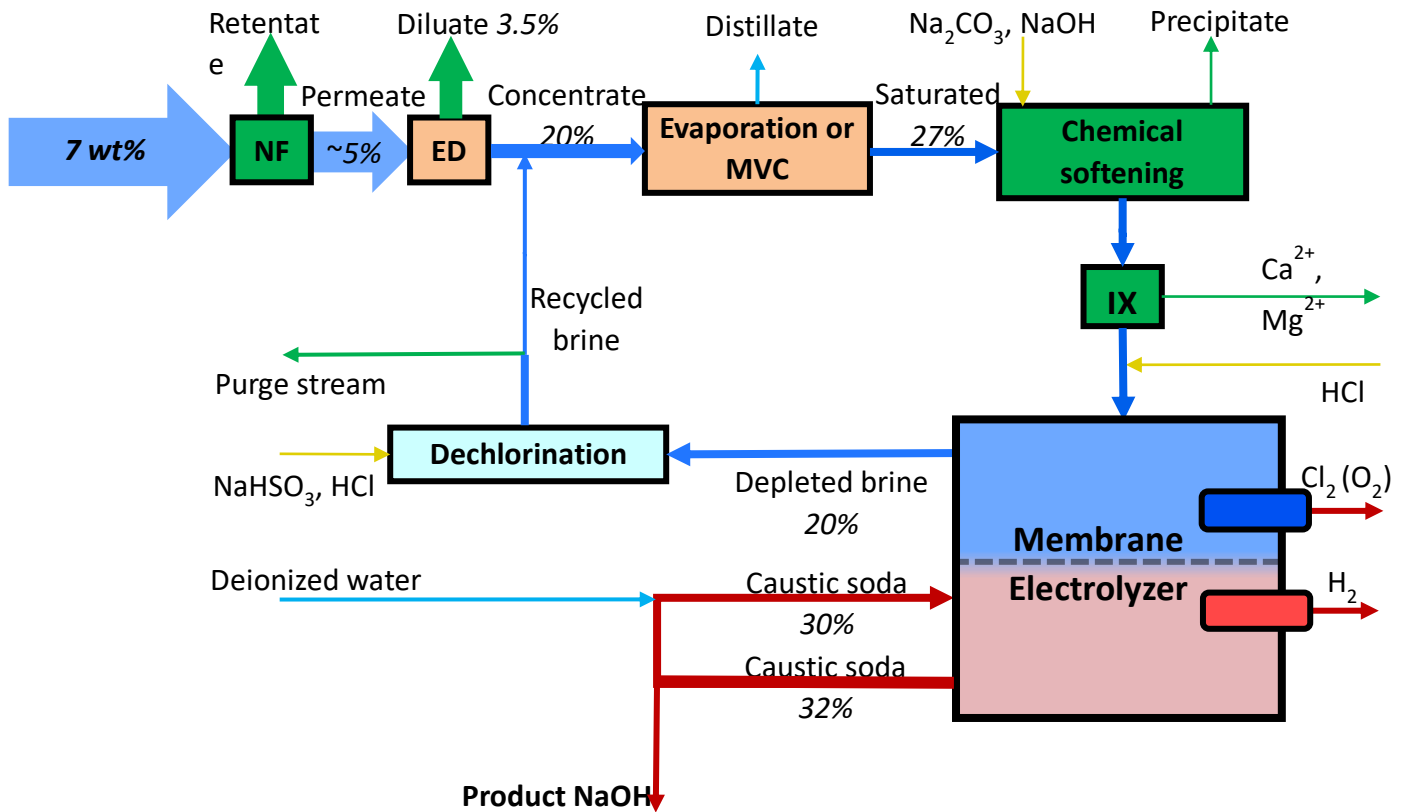
- 598  
599 (40) Song, Y.; Chen, C.-C. Symmetric electrolyte nonrandom two-liquid activity coefficient model.  
600 *Ind. Eng. Chem. Res.* **2009**, *48* (16), 7788–7797.  
601
- 602 (41) Aspen Technology Inc., Benefits of multi-solvent NRTL models in Aspen Plus. Technical  
603 Report Aspen Technology Inc., 2012.  
604
- 605 (42) Warsinger, D. M.; Tow, E. W.; Swaminathan, J.; Lienhard J. H. Theoretical framework for  
606 predicting inorganic fouling in membrane distillation and experimental validation with  
607 calcium sulfate. *J. Membrane Sci.* **2017**, *528*, 381–390.  
608
- 609 (43) Roy, Y.; Warsinger, D. M.; Lienhard, J. H. Effect of temperature on ion transport in  
610 nanofiltration membranes: Diffusion, convection and electromigration. *Desalination* **2017**,  
611 *420*, 241–257.  
612
- 613 (44) Warsinger, D. M.; Servi, A.; Van Belleghem, S.; Gonzalez, J.; Swaminathan, J.; Kharraz, J.;  
614 Chung, H. W.; Arafat, H. A.; Gleason, K. K.; Lienhard, J. H. Combining air recharging and  
615 membrane superhydrophobicity for fouling prevention in membrane distillation. *J.*  
616 *Membrane Sci.* **2016**, *505*, 241–252.  
617
- 618 (45) Warsinger, D. M.; Tow, E. W.; Maswadeh, L. A.; Connors, G.; Swaminathan, J.; Lienhard J. H.  
619 Inorganic fouling mitigation by salinity cycling in batch reverse osmosis. *Water Res.* **2018** (in  
620 press) <https://doi.org/10.1016/j.watres.2018.01.060>.  
621
- 622 (46) Asahi Glass and Chemicals Co., *Personal Communication to Kishor G. Nayar*, October 2016.  
623
- 624 (47) Leitz, F. B. Electrodialysis for industrial water cleanup. *Environ. Sci. Technol.* **1976**, *10* (2),  
625 136–139.  
626
- 627 (48) Mousavi, S. E.; Moosavian, S. M. A.; Jalali, M.; Zahedi, P.; Karimi, E. Sulfate removal from  
628 chlor-alkali brine using nanofiltration: Parameters investigation and optimization via  
629 Taguchi design method. *Desalin. Water Treat.* **2017**, *100*, 75-90.  
630
- 631 (49) Mirzazadeh, T.; Mohammadi, F.; Soltanieh, M.; Joudaki, E. Optimization of caustic current  
632 efficiency in a zero-gap advanced chlor-alkali cell with application of genetic algorithm  
633 assisted by artificial neural networks. *Chem. Eng. J.* **2008**, *140* (1-3), 157–164.  
634
- 635 (50) Jalali, A.; Mohammadi, F.; Ashrafizadeh, S. Effects of process conditions on cell voltage,  
636 current efficiency and voltage balance of a chlor-alkali membrane cell. *Desalination* **2009**,  
637 *237* (1-3), 126–139.  
638
- 639 (51) Walha, K.; Amar, R. B.; Quemeneur, F.; Jaouen, P. Treatment by nanofiltration and reverse  
640 osmosis of high salinity drilling water for seafood washing and processing abstract.  
641 *Desalination* **2008**, *219* (1-3), 231–239.

- 642  
643 (52) Liu, J.; Yuan, J.; Ji, Z.; Wang, B.; Hao, Y.; Guo, X. Concentrating brine from seawater  
644 desalination process by nanofiltration–electrodialysis integrated membrane technology.  
645 *Desalination* **2016**, *390*, 53–61.  
646  
647 (53) Dow Water & Process Solutions, Design Software: ROSA (Reverse Osmosis System Analysis).  
648 <http://www.dow.com/en-us/water-and-process-solutions/resources/design-software>  
649 (revised on 2017.08.29).  
650  
651 (54) Dow Water & Process Solutions, ROSA Help File.  
652 [https://dowac.custhelp.com/app/answers/detail/a\\_id/205](https://dowac.custhelp.com/app/answers/detail/a_id/205) (revised on 2017.08.29).  
653  
654 (55) Dow Water & Process Solutions, Amberlite™ selective resins for brine purification in the  
655 chlor-alkali industry, Technical Report Dow Water & Process Solutions.  
656  
657 (56) Lienhard, J. H.; Mistry, K. H.; Sharqawy, M. H.; Thiel, G. P. Thermodynamics, Exergy, and  
658 Energy Efficiency in Desalination Systems. In *Desalination Sustainability: A Technical,*  
659 *Socioeconomic, and Environmental Approach*, Chpt. 4, H. A. Arafat, ed. Elsevier Publishing  
660 Co., **2017**.  
661  
662 (57) Swaminathan, J.; Chung, H. W.; Warsinger, D. M.; Lienhard, J. H. Energy efficiency of  
663 membrane distillation up to high salinity: Evaluating critical system size and optimal  
664 membrane thickness. *Appl. Energ.* **2018**, *211*, 715-734.  
665  
666 (58) Kumar, A.; Katherine, G.; Thiel, G.; Schroder, U.; Lienhard, J. H. Direct electro-synthesis of  
667 sodium hydroxide and hydrochloric acid from brine streams. *Nature Catalysis* **2018**, in  
668 revision following review.  
669  
670 (59) *Electric power monthly with data for October 2017*.  
671 <https://www.eia.gov/electricity/monthly/archive/december2017.pdf> (Table 5.6.A., Revised  
672 on 2018.02.04).  
673  
674 (60) *Natural gas weekly update*. <https://www.eia.gov/naturalgas/weekly> (Revised on  
675 2018.02.04).  
676  
677 (61) *Indicative Chemical Prices A-Z*. <https://www.icis.com/chemicals/channel-info-chemicals-a-z>  
678 (Revised on 2018.02.04).  
679  
680 (62) Santana, M. V.; Zhang, Q.; Mihelcic, J. R. Influence of water quality on the embodied energy  
681 of drinking water treatment. *Environ. Sci. Technol.* **2014**, *48* (5), 3084–3091.  
682

683 TOC figure



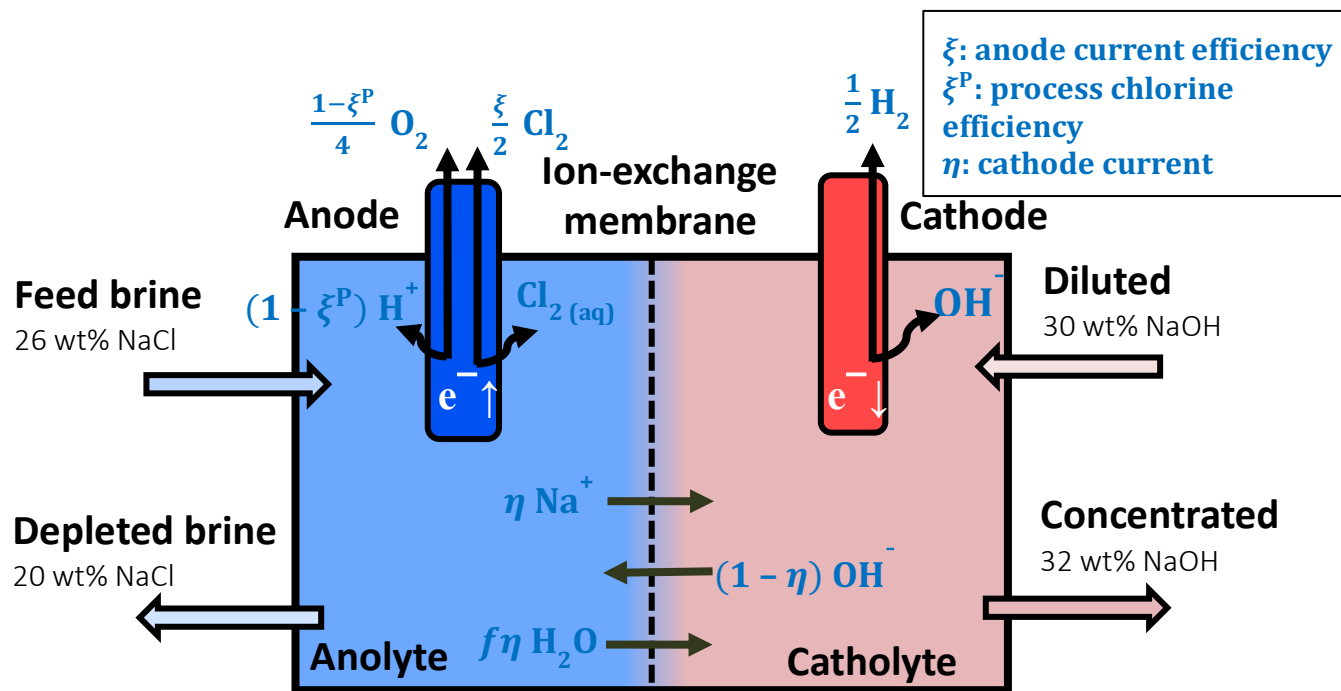
684



685

686 **Figure 1.** Brine to NaOH system block flow diagram for this study. Successive components purify  
 687 (green) or concentrate (orange) the feed to reach suitable input conditions for a membrane  
 688 electrolyzer. Typical brine and caustic concentrations are shown (percentage given as wt% solute).  
 689 Color key of streams: Dark blue = brine streams; light blue = water; red = product; yellow = chemical  
 690 dosage; green = effluent. Width of arrows indicates the mass flows. Starting from the inlet (left to  
 691 right), the successive process includes nanofiltration (NF), electrodialysis (ED), evaporation or  
 692 mechanical vapor compression (MVC), chemical softening, and ion-exchange (IX) as pretreatment  
 693 components; the last step is the membrane electrolyzer as the NaOH production unit, with  
 694 dechlorination as a post-treatment step. Components are chosen for purification capabilities (by  
 695 concentration) and energy efficiency for concentration steps. Membrane electrolysis produce the  
 696 primary product (NaOH) as well as the gases Cl<sub>2</sub> and H<sub>2</sub> at the electrodes.

697

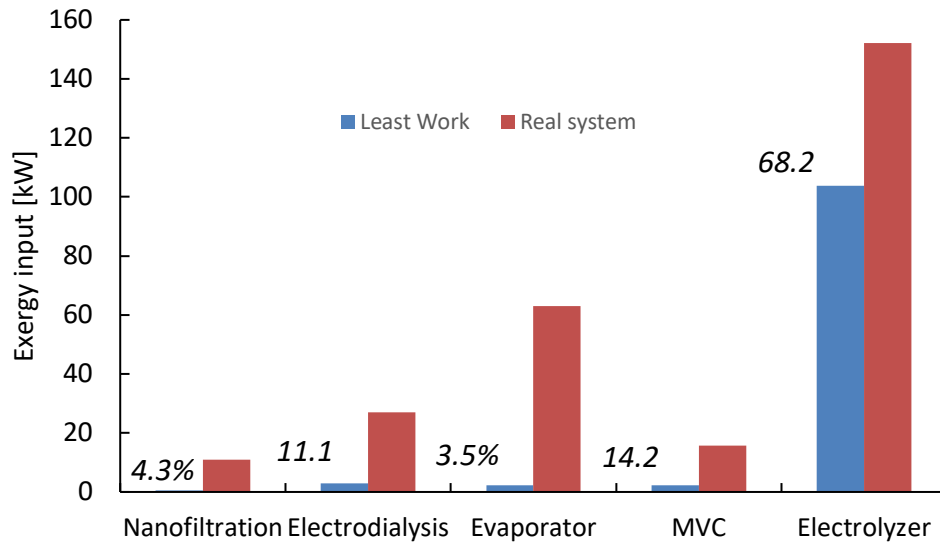


699

700 **Figure 2.** Schematic diagram of a typical cell for the chlor-alkali process, containing an ion-exchange  
 701 membrane as well as anode and cathode for the reaction. The ion-exchange membrane separates the  
 702 anode (left, blue) and the cathode chamber (right, red). Black arrows in the figure show species  
 703 transported through the membrane and generated at the electrodes. Molar amount of species (blue  
 704 formulas) are based on 1 mole of electrons (1 Faraday) consumed by the electrolyzer.

705

706

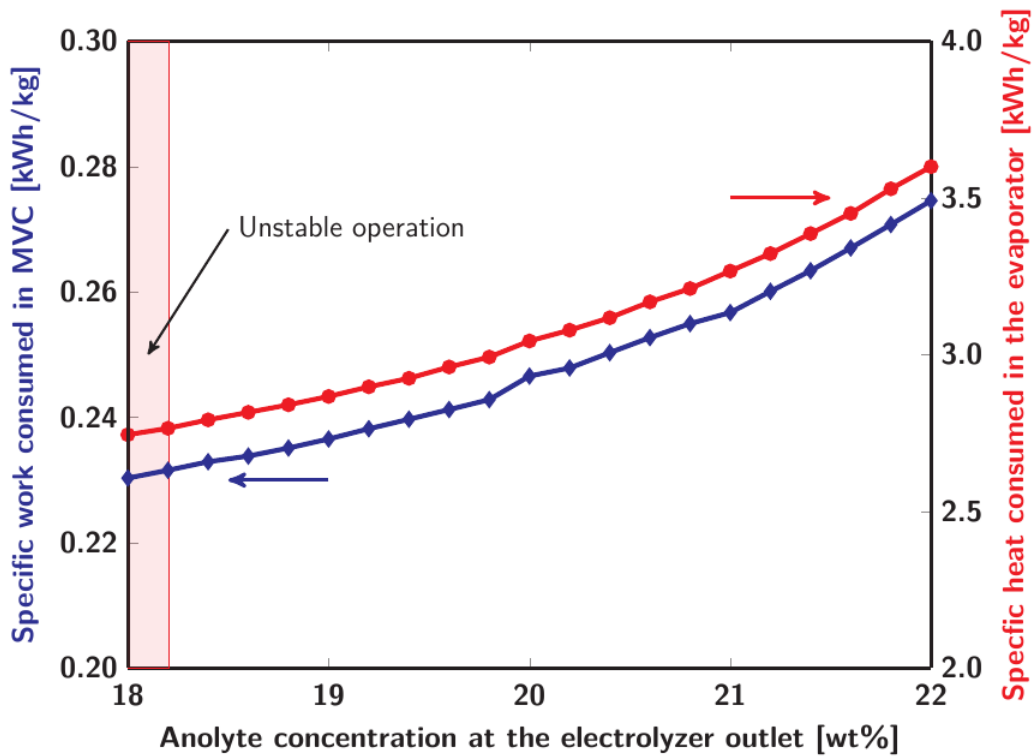


707

708 **Figure 3.** Least work compared to total consumed exergy (denominator in equation (2)) in the  
 709 nanofiltration, electrodialysis, evaporation, MVC, and electrolyzer components. Percentages given are  
 710 second law efficiencies (least work divided by actual exergy consumption).

711

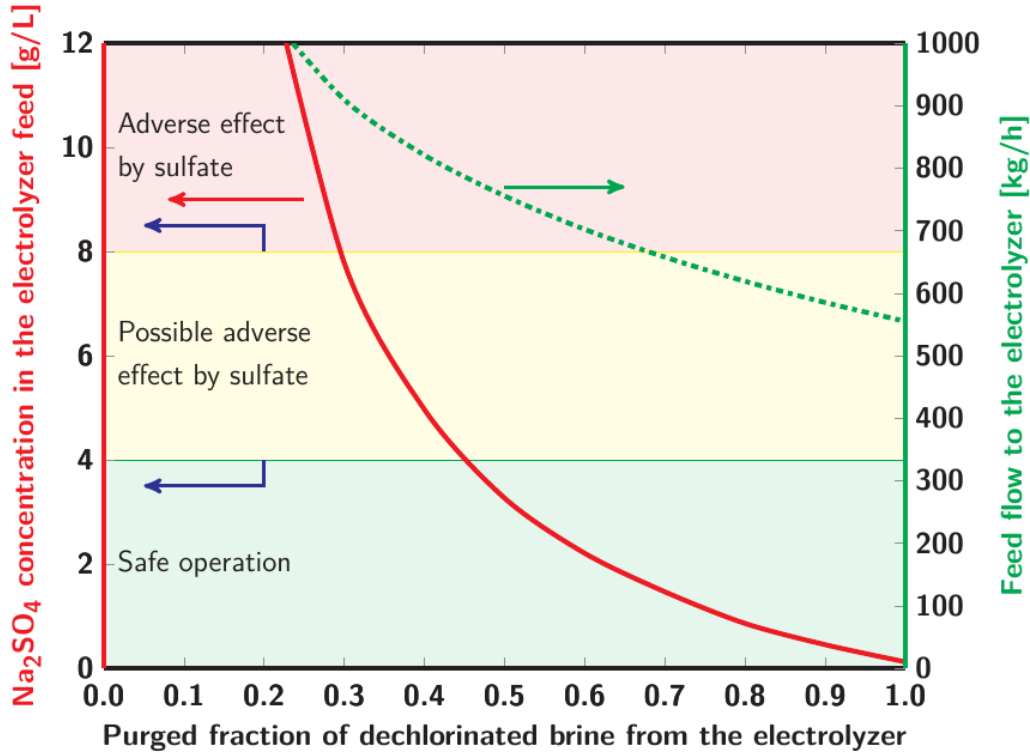
712



713

714 **Figure 4.** Evaporator (right, red) and MVC (left, blue) energy consumption normalized by the caustic  
 715 production amount (as 32 wt% solution) with respect to the anolyte outlet concentration of the  
 716 electrolyzer. A stable operation of the membrane electrolyzer is no longer feasible with anolyte  
 717 concentration lower than 18.2 wt% (red zone).

718



719

720 **Figure 5.** Impact of depleted brine purge on brine flow into electrolyzer and sulfate accumulation in  
 721 the cell. Red and yellow zones indicate that the sulfate concentration exceeds tolerance in most  
 722 membrane cells ( $> 8$  g/L  $\text{Na}_2\text{SO}_4$ ), or some membrane cells ( $> 4$  g/L  $\text{Na}_2\text{SO}_4$ ), respectively.<sup>28,31,32</sup> Green  
 723 zone is free of adverse effects of sulfate.

724

725 **Table 1.** Selected modeling parameters and their values of the final system-level process.

Component	Parameter	Value	Unit	Source/Rationale
Feed brine	Temperature	25	°C	Ambient
	Mass fraction $\text{H}_2\text{O}$	91.87	%	Boundary condition.
	Mass fraction $\text{NaCl}$	6.39	%	Corresponds to 0.69 g/L $\text{Ca}^{2+}$ , 2.2 g/L
	Mass fraction $\text{CaCl}_2$	0.18	%	$\text{Mg}^{2+}$ , 5.3 g/L $\text{SO}_4^{2-}$ , 85 mg/L $\text{Br}^-$ (based on
	Mass fraction $\text{MgCl}_2$	0.81	%	density of 1059 kg/m <sup>3</sup> calculated by
	Mass fraction $\text{Na}_2\text{SO}_4$	0.74	%	Aspen).
	Mass fraction $\text{NaBr}$	0.01	%	

				2.75 wt% as Na <sup>+</sup> is the stoichiometric amount of typical 7.0 wt% SWRO brine
Nanofiltration	Temperature	26	°C	Isothermal, temperature after pumping is 25.6 °C
	Pressure feed	20	bar	Typical value for high-salinity feeds <sup>36,51,52</sup>
	Water recovery	30.3	%	
	Rejection of Cl <sup>-</sup>	16.1	%	ROSA Simulation <sup>53,54</sup> : Two-stage system with six NF270-400 elements per stage, see SI “Nanofiltration”
	Rejection of SO <sub>4</sub> <sup>2-</sup>	95.7	%	
	Rejection of Ca <sup>2+</sup>	38.3	%	
	Rejection of Mg <sup>2+</sup>	40.1	%	
	Rejection of Br <sup>-</sup>	16.1	%	Assumed same as Cl <sup>-</sup>
Pump efficiency	80	%	Estimation	
Electrodialysis (C: concentrate, D: diluate)	Temperature	26	°C	Assumed isothermal
	Outlet concentration C	20	wt%	Industrial upper limit <sup>46</sup>
	Outlet concentration D	3.5	wt%	Can be fed back to RO plant
Evaporator	Temperature	108	°C	Brine temperature at 1 bar with saturated NaCl
	Brine concentration outlet	27	wt%	Ensure saturated brine for the electrolyzer
Chemical Softening	Temperature	60	°C	High enough to speed up the precipitation process (source IPPC, cited by Garriga <sup>36</sup> same as ion exchange)
Ion exchange	Temperature	60	°C	Recommended temperature <sup>55</sup>
Electrolyzer	Temperature	88	°C	Reference plant <sup>28</sup>
	Pressure anolyte	1.09	bar	Reference plant <sup>28</sup>
	Pressure catholyte	1.05	bar	Reference plant <sup>28</sup>
	Feed brine pH value	3	-	See SI “Anode and cathode current efficiencies in electrolyzer”
	Product NaOH concentration	32	wt%	Reference plant <sup>28</sup>
	Recycle NaOH concentration	30.3	wt%	Reference plant <sup>28</sup>
	Cathode current efficiency	94	%	Reference plant <sup>28</sup>
	Anode current efficiency	96	%	Estimation
	Water transport number	4.25	-	Reference plant <sup>28</sup>
	Anolyte outlet concentration	19	wt%	See section “Anolyte outlet concentration”

	Voltage of the electrolyzer	3.2	V	Reference plant <sup>28</sup>
Purge splitter	Purge ratio	0.5	-	See section "Purge ratio"
Dechlorination	Temperature	88	°C	Adiabatic mixing

726

727

728 **Table 2.** Estimated operation expenditures of the purposed system. Cost normalized by the caustic  
729 production of 64.8 kg/h.

Component	Consumption	Cost per unit	Cost per produced NaOH
NF	10.9 kW electricity	0.0695 \$/kWh <sup>59</sup>	0.0117 \$/kg
ED	26.8 kW electricity	0.0695 \$/kWh <sup>59</sup>	0.0288 \$/kg
Electrolyzer	152.1 kW electricity	0.0695 \$/kWh <sup>59</sup>	0.1631 \$/kg
Evaporator/ MVC	190.8 kW heat / 15.8 kW electricity	0.0102 \$/kWh (based on natural gas price <sup>60</sup> / 0.0695 \$/kWh <sup>59</sup> )	0.0301 \$/kg 0.0169 \$/kg
Chemical softening	16.2 kg/h Na <sub>2</sub> CO <sub>3</sub> (3.6 wt%)	0.165 \$/kg dry <sup>61</sup>	0.0014 \$/kg
Ion-exchange	0.154 kg/h HCl (6 wt%)	0.243 \$/kg (dry base) <sup>61</sup>	<0.0001 \$/kg
Acidifier	1.356 kg/h HCl (37 wt%)	0.243 \$/kg (dry base) <sup>61</sup>	0.0018 \$/kg
Dechlorination	4.321 kg/h NaHSO <sub>3</sub> (38 wt%)	0.529 \$/kg dry <sup>61</sup>	0.0130 \$/kg
TOTAL			0.2501 \$/kg (Evaporator) 0.2369 \$/kg (MVC)

730